Technion - Israel Institute of Technology

Numerical Methods in Aeronautical Engineering (086172)

GRADE	OUT OF	CHAPTER
	2	ABSTRACT
	2	CONTENTS, STYLE &C.
	4	PHYSICAL PROBLEM
	4	MATHEMATICAL MODEL
	26	NUMERICAL METHODS
	20	INFLUENCE OF NUMERICAL METHODS
	20	RESULTS
	2	SUMMARY & CONCLUSIONS
	20	COMPUTER PROGRAM
	100	**TOTAL**

Daniel Engelsman, ID 300546173 @ September 18, 2019

= Final Project # 3 =

Contents

List of Figures

1 Abstract

In this project I would like to examine the flow regime that is generated by a fluid profile that is entering a channel at one side, and leaves it with a fully developed flow by the exit. To simplify the model, we will analyze it as a 2D problem in space, incompressible but viscid varying two values of Re numbers.

2 The physical problem

Consider a 2D profile of an L long channel that is opened at **AH**, narrows at **F** and exits at **BC**. The viscous fluid enters horizontally ($u_0(y)$, $\cancel{v_0}^{0}$) and leaves fully developed such that its velocity vector will exhibit parabolic distribution.

Provided that the Re numbers are relatively small, we should expect getting a laminar ($Re \leq 2,040$) and non-turbulent flow in most of the cavity, apart from the line of symmetry, where counter direction flow might collide.

I shall look for suspicious areas across the problem's shape in sought of influential factors that increase sensitivity (numerical / physical).

3 The mathematical model

Using Navier-Stokes equations, we'll write the governing equations for the steady-state ($\frac{\partial f}{\partial t} = 0$), incompressible ($\frac{\partial \rho}{\partial t} = 0$) fluid flow problem, where $\nabla \bar{p} \to 0$ and no external force :

$$\text{Continuity :} \qquad \frac{\partial u}{\partial x} + \frac{\partial v}{\partial y} = 0 \tag{3.1}$$

The momentum balance equation in a conservation form :

$$\frac{\partial}{\partial t}(\rho \mathbf{u}) + \nabla \cdot (\rho \mathbf{u} \times \mathbf{u}) = -\nabla \bar{p} + \mu \nabla^2 \mathbf{u} + \frac{1}{3}\mu \nabla(\nabla \cdot \mathbf{u}) + \rho g \tag{3.2}$$

and momentum of each flow component where $u \parallel \hat{x}$ and $v \parallel \hat{y}$:

$$\hat{x} \ : \qquad \frac{\partial u}{\partial t} + \frac{\partial u}{\partial x}u + \frac{\partial u}{\partial y}v = \frac{\mu}{\rho}\Big(\frac{\partial^2 u}{\partial x^2} + \frac{\partial^2 u}{\partial y^2}\Big) \tag{3.3}$$

$$\hat{y} \ : \qquad \frac{\partial v}{\partial t} + \frac{\partial v}{\partial x}u + \frac{\partial v}{\partial y}v = \frac{\mu}{\rho}\Big(\frac{\partial^2 v}{\partial x^2} + \frac{\partial^2 v}{\partial y^2}\Big) \tag{3.4}$$

Using stream function - vorticity formulation, we can present the following terms :

$$\text{Velocity components :} \qquad u = \frac{\partial \psi}{\partial y} \ , \quad v = -\frac{\partial \psi}{\partial x} \tag{3.5}$$

$$\text{Define vorticity :} \qquad \omega = \frac{\partial u}{\partial y} - \frac{\partial v}{\partial x} \tag{3.6}$$

$$\text{plug } u(\psi),\, v(\psi) : \qquad \omega = \frac{\partial^2 \psi}{\partial y^2} + \frac{\partial^2 \psi}{\partial x^2} \tag{3.7}$$

After fair amount of arithmetic manipulations, we get <u>another</u> elliptic equation :

$$\text{Stream function} \ : \qquad \frac{\partial \omega}{\partial t} + \frac{\partial \omega}{\partial x}u + \frac{\partial \omega}{\partial y}v = \frac{\mu}{\rho}\Big(\frac{\partial^2 \omega}{\partial x^2} + \frac{\partial^2 \omega}{\partial y^2}\Big) \tag{3.8}$$

Eq. **3.7** is elliptic w.r.t ψ, and Eq. **3.8** is parabolic w.r.t time (in the unsteady-state case), such that both are coupled, and can be solved as displayed in the flowchart :

$$\begin{aligned}
(i) \qquad \hat{\omega}(\Delta t) &= f(u, v) \\
(ii) \qquad \hat{\psi} &= f(\hat{\omega}) \\
(iii) \qquad \hat{u},\ \hat{v} &= f(\hat{\psi}) \quad \Rightarrow \quad \text{Return to } (i)
\end{aligned}$$

For the sake of convenience we'll express the equations in a non-dimensional form :

$$\tilde{x} = \frac{x}{L} \ , \ \tilde{y} = \frac{y}{L} \ , \ \tilde{u} = \frac{u}{L} \ , \ \tilde{v} = \frac{v}{L} \ , \ \tilde{\omega} = \frac{\omega}{U_0/L} \ , \ \tilde{\psi} = \frac{\psi}{U_0 L} \ , \ Re = \frac{UL}{\nu} \tag{3.9}$$

And divide the functions by L, such that get the following normalized equations :

$$\text{Voritcity function} \ : \qquad \frac{\partial\tilde{\omega}}{\partial t} + \frac{\partial\tilde{\omega}}{\partial\tilde{x}}\tilde{u} + \frac{\partial\tilde{\omega}}{\partial\tilde{y}}\tilde{v} = \frac{1}{Re}\Big(\frac{\partial^2\tilde{\omega}}{\partial\tilde{x}^2} + \frac{\partial^2\tilde{\omega}}{\partial\tilde{y}^2}\Big) \tag{3.10}$$

$$\text{Stream function} \ : \qquad \frac{\partial^2\tilde{\psi}}{\partial\tilde{x}^2} + \frac{\partial^2\tilde{\psi}}{\partial\tilde{y}^2} = \tilde{\omega} \tag{3.11}$$

$$\text{Velocity components} \ : \qquad \tilde{u} = \frac{\partial\tilde{\psi}}{\partial\tilde{y}} \ , \ \tilde{v} = -\frac{\partial\tilde{\psi}}{\partial\tilde{x}} \tag{3.12}$$

For presentation convenience, the notation ($\tilde{\cdot}$) will be dismissed from here on.

3.1 Initial and boundary conditions

Given the problem's geometry we can portray the full symmetry as such :

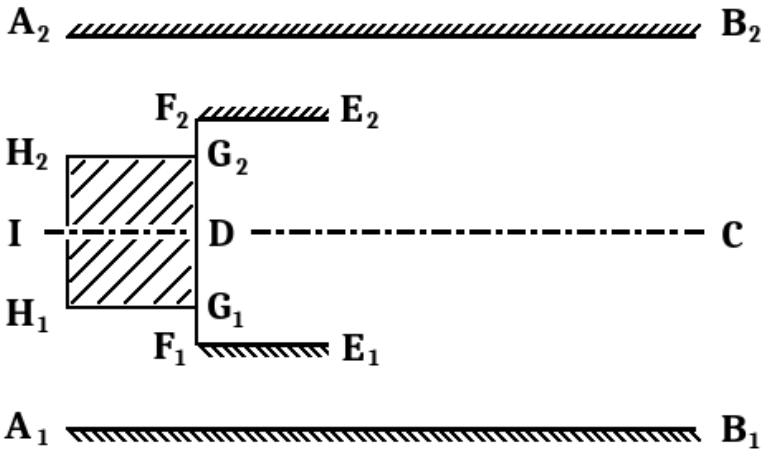

Figure 1: Full geometry shape of the problem

Let A_1 coincide with the origin $(0,\ 0)$, and flow enter horizontally from A_1A_2 entrance, and advances towards B_1B_2 exit. The problem's nature allows assuming symmetry around IDC line, such that it's suffice to analyze only one chosen half.

All the solid walls satisfy two important conditions ($u = v = 0$) :

$$(i)\ \text{No-penetration} \qquad (ii)\ \text{No-slip} \tag{3.13}$$

The solid walls satisfy conditions **3.13**, such that the boundary layer diffuses vorticity into the free fluid, and can be expressed using *Taylor expansion* :

$$\psi_{i,\mathrm{w}\pm\Delta x} = \psi_{\mathrm{w}} \pm \Delta x \cancelto{0}{\frac{\partial \psi}{\partial y}} + \frac{\Delta x^2}{2}\Big(\frac{\partial^2 \psi}{\partial y^2}\Big)_{=\omega} + O(\Delta x^3) \tag{3.14}$$

$$\omega_{i,\mathrm{w}} = 2 \cdot \frac{\psi_{\mathrm{w}\pm\Delta y} - \psi_{i,\mathrm{w}}}{\Delta x^2} + O(\Delta x) \tag{3.15}$$

Conveniently set $\psi_{A_1} = 0$, we get the following set of boundary conditions :

Segment	Indices	$\mathbf{u}$	$\mathbf{v}$	ψ	ω
$A_1H_1^{in}$	$i = 1\ ,\ 1 \le j \le \frac{L/20}{\Delta y}$	$u_{in}(y)$	0	$\int_{y_{A_1}}^{y_{A_1}+j\Delta y} u_{in}(y)\ dy$	$\frac{\partial u_{in}}{\partial y} - \cancelto{0}{\frac{\partial v_{in}}{\partial x}}$
H_1G_1	$1 \le i \le \frac{2L/20}{\Delta x},\ j = \frac{L/20}{\Delta y}$	0	0	$\int_{y_{A_1}}^{y_{H_1}} u_{in}(y)\ dy$	$\frac{2}{\Delta_y^2}\big(\psi_{\frac{L}{20}-\Delta y} - \psi_{\frac{L}{20}}\big)$
$G_1^-F_1$	$i = \Big\lfloor \frac{2L/20}{\Delta x} \Big\rfloor,\ \frac{L/40}{\Delta y} \le j \le \frac{2L/40}{\Delta y}$	0	0	$\psi_{H_1G_1}$	$\frac{2}{\Delta_x^2}\big(\psi_{\frac{L}{10}-\Delta x} - \psi_{\frac{L}{10}}\big)$
$F_1E_1^-$	$\frac{2L/20}{\Delta x} \le i \le \frac{3L/20}{\Delta x},\ j = \Big\lfloor \frac{L/40}{\Delta y} \Big\rfloor$	0	0	$\psi_{G_1^-F_1}$	$\frac{2}{\Delta_y^2}\big(\psi_{\frac{L}{40}-\Delta y} - \psi_{\frac{L}{40}}\big)$
$F_1E_1^+$	$\frac{2L/20}{\Delta x} \le i \le \frac{3L/20}{\Delta x}\ , j = \Big\lceil \frac{L/40}{\Delta y} \Big\rceil$	0	0	$\psi_{F_1E_1^-}$	$\frac{2}{\Delta_y^2}\big(\psi_{\frac{L}{40}+\Delta y} - \psi_{\frac{L}{40}}\big)$
F_1^+D	$i = \Big\lceil \frac{2L/20}{\Delta x} \Big\rceil,\ \frac{L/40}{\Delta y} \le j \le \frac{6L/20}{\Delta y}$	0	0	$\psi_{F_1E_1^+}$	$\frac{2}{\Delta_x^2}\big(\psi_{\frac{L}{10}+\Delta x} - \psi_{\frac{L}{10}}\big)$
DC^{Sym}	$\Big\lceil \frac{2L/20}{\Delta x} \Big\rceil \le i \le \frac{L}{\Delta x},\ j = \frac{6L/20}{\Delta y}$	$f_{extr.}$	0	$\psi_{F_1^+D} = \text{const.}$	0
B_1C^{Out}	$i = \frac{L}{\Delta x}\ ,\ 1 \le j \le \frac{6L/20}{\Delta y}$	$u_{out}(y)$	0	$\cancelto{0}{\psi_{B_1}} + \int_{y_{B_1}}^{y_C} u_{out}(y)$	$\frac{\partial u_{out}}{\partial y} - \cancelto{0}{\frac{\partial v_{out}}{\partial x}}$
$A_1B_1^{Base}$	$1 \le i \le L,\ j = 1$	0	0	$\psi_{A_1} = \psi_{B_1} = 0$	$\frac{2}{\Delta_y^2}\big(\psi_{i,2} - \psi_{i,1}\big)$

3.2 Inlet and outlet formulation

The last challenge is defining the velocity profiles developed in the inlet, outlet and the symmetry line. Starting from contuity equation for incompressible flow :

$$\nabla \bar{U} = 0 \;\Rightarrow\; \cancelto{0}{\frac{\partial u}{\partial x}} + \frac{\partial v}{\partial y} = 0 \;\Rightarrow\; v = v(y=0)_{\text{const.}} \tag{3.16}$$

Momentum balance in $\hat{x}$ direction :

$$\cancelto{0}{\frac{\partial u}{\partial t}} + \cancelto{0}{\frac{\partial u}{\partial x}}u + \cancelto{0}{\frac{\partial u}{\partial y}}v = -\frac{1}{\rho}\frac{\partial p}{\partial x} + \frac{\mu}{\rho}\Big(\cancelto{0}{\frac{\partial^2 u}{\partial x^2}} + \frac{\partial^2 u}{\partial y^2}\Big) \tag{3.17}$$

$$\mu\frac{\partial^2 u}{\partial y^2} = \frac{\partial p}{\partial x} = \text{const.} = c \quad \Rightarrow \quad u(y) = \frac{c}{2}y^2 + dy + e \tag{3.18}$$

We got a general expression for the developed velocity. Now we would like to taylor it each of the orifices, starting with $u_{in}(y)$ entering the inlet :

$$\text{Parabolic dist. :} \quad u_{in}(0) = 0 \;\Rightarrow\; e = 0\;; \quad u_{in}(\frac{L}{20}) = 0 \;\Rightarrow\; d = -\frac{cL}{40};$$
$$\text{Maximal flow normalized :} \quad u_{in}(\frac{L}{40}) = \mathbf{1} \;\Rightarrow\; c = -2(\frac{40}{L})^2 = -8$$

And we get the following profiles at the inlet :

$$u_{in}(y) = -4y^2 + 4y \tag{3.19}$$

$$\psi_{in}(y) = \cancelto{0}{\psi_{A_1}} + \int_0^y u_{in}(y)\; dy = \Big[-\frac{4}{3}y^3 + 2y^2 \Big|_0^y \tag{3.20}$$

$$\omega_{in}(y) = \frac{\partial u_{in}}{\partial y} - \cancelto{0}{\frac{\partial v_{in}}{\partial x}} = -8y + 4 \tag{3.21}$$

And similar analysis for the outlet, starting with its parabolic properties :

$$u_{out}(0) = 0 \;\Rightarrow\; e = 0\;; \quad u'_{out}(\frac{6L}{20}) = 0 \;\Rightarrow\; d = -\frac{6cL}{20} = -6c;$$

Assuming mass flux conservation from both sides (lower symmetric half) :

$$\dot{m}_{in} = \dot{m}_{out} \quad \Leftrightarrow \quad \rho b \int_0^{L/20} u_{in}(y)\ dy = \rho b \int_0^{6L/20} u_{out}(y)\ dy$$

$$\frac{2}{3}\rho b = \rho b \int_0^{6L/20} (\frac{c}{2}y^2 - 6cy)\ dy \quad \Rightarrow \quad \frac{2}{3} = c\left[\frac{1}{6}y^3 - 3y^2\right|_0^6 \quad \Rightarrow \quad c = -\frac{1}{108}$$

And we get the following profiles at the outlet :

$$u_{out}(y) = -\frac{1}{216}y^2 + \frac{1}{18}y \tag{3.22}$$

$$\psi_{out}(y) = \cancelto{0}{\psi_{B_1}} + \int_0^y u_{out}(y)\ dy = \left[-\frac{1}{648}y^3 + \frac{1}{9}y^2\right|_0^y \tag{3.23}$$

$$\omega_{out}(y) = \frac{\partial u_{out}}{\partial y} - \cancelto{0}{\frac{\partial v_{out}}{\partial x}} = -\frac{1}{108}y + \frac{1}{18} \tag{3.24}$$

At last we can draw a figurative profile of the flow domain as such :

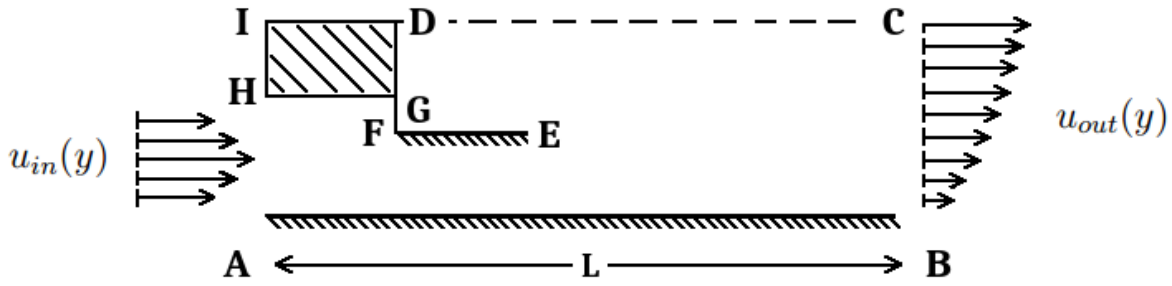

Figure 2: Half geometry of the problem around the line of symmetry (IDC)

Where inlet velocity at **AH** is normalized to '1' in its half height, and exits as a half parabola on **BC**.

4 The numerical method

Both functions after being discretized supply their own set of equations, but solved differently. We'll express both using finite differences (=**F.D**) on the $x-y$ plane as follows :

$$\begin{aligned} x = i \cdot \Delta x \qquad \forall \qquad i \ = \ 1, \ \ldots, \ N+1 \ \Leftrightarrow \ [0 \ , \ L/\Delta x] \\ y = j \cdot \Delta y \qquad \forall \qquad j \ = \ 1, \ \ldots, \ M+1 \ \Leftrightarrow \ [0 \ , \ \frac{6L}{20}/\Delta y] \end{aligned}$$

4.1 Stream function

The stream function (Eq. **3.8**) can be solved by a suitable elliptic method, such as implicit *Guass Seidel*, as already seen in previous homeworks :

$$\textbf{PDE :} \qquad \nabla^2\psi = \frac{\partial^2\psi}{\partial y^2} + \frac{\partial^2\psi}{\partial x^2} = \omega \tag{4.1}$$

$$\textbf{F.D :} \qquad \frac{\psi_{i+1,j} - 2\psi_{i,j} + \psi_{i-1,j}}{\Delta x^2} + \frac{\psi_{i,j+1} - 2\psi_{i,j} + \psi_{i,j-1}}{\Delta y^2} = \omega_{i,j} \tag{4.2}$$

After sorting and extracting the $\psi_{i,j}$ diagonal, we get the following iterative method :

$$\psi^{(n+1)}_{i,j\ (GS)} = \frac{\Delta y^2\Big(\psi^{(n)}_{i+1,j} + \psi^{(n+1)}_{i-1,j}\Big) + \Delta x^2\Big(\psi^{(n)}_{i,j+1} + \psi^{(n+1)}_{i,j-1}\Big) - \Delta x^2\Delta y^2\omega^{(n)}_{i,j}}{2\Big(\Delta x^2 + \Delta y^2\Big)} \ \Bigg|^{i=1,\ldots,N}_{j=1,\ldots,M} \tag{4.3}$$

The local truncation error is $O(\Delta x^2, \Delta y^2)$, and to ensure convergence we'll use the S.O.R :

$$\psi^{(n+1)}_{i,j} = \psi^{(n)}_{i,j} + \Omega_{opt}\Big(\psi^{(n+1)}_{i,j\ (GS)} - \psi^{(n)}_{i,j}\Big) \tag{4.4}$$

The optimal solution of Ω_{opt} is fully developed in the course papers, so it will suffice to bring the final solution of the method's $\underline{a}_{i,j}$ block matrix and λ's eigenvalues :

$$\Omega_{opt} = \frac{2\Big(1 - \sqrt{1-\mu^2}\Big)}{\mu^2} \quad , \quad \mu = \frac{1}{2}\Big[\cos(\frac{\pi}{M+1}) + \cos(\frac{\pi}{N+1})\Big] \tag{4.5}$$

The chosen convergence criterion will be a simple absolute error : $\Big|\psi^{(n+1)}_{i,j} - \psi^{(n)}_{i,j}\Big| < \epsilon$.

4.2 Vorticity function

The vorticity function (Eq. **3.10**) can be solved using *1st order upwind differences* method, where the transport elements are written in accordance with u, v sign. Divided into 4 possible cases expressed in **F.D**, note that the (u, v) sign corresponds to $(\pm, \mp)$:

$$u_{i,j} > 0 \quad \cap \quad \begin{cases} v_{i,j} > 0 \\ v_{i,j} < 0 \end{cases} :$$

$$\omega_{i,j}^{(k+1)} = \omega_{i,j}^{(k)} + \Delta t \Bigg[\Delta y^2 \omega_{i+1,j} + \omega_{i-1,j}\big(\Delta y^2 + Re\Delta x \Delta y^2 u_{i,j}\big) + \Delta x^2 \omega_{i,j\pm1} + \dots$$

$$\dots + \omega_{i,j\mp1}\big(\Delta x^2 \pm Re\Delta y \Delta x^2 v_{i,j}\big) + \omega_{i,j}\Big(\mp Re\Delta y \Delta x^2 v_{i,j} - Re\Delta x \Delta y^2 u_{i,j} - 2\Delta y^2 - 2\Delta x^2 \Big) \Bigg]$$

And similarly,

$$u_{i,j} < 0 \quad \cap \quad \begin{cases} v_{i,j} > 0 \\ v_{i,j} < 0 \end{cases} :$$

$$\omega_{i,j}^{(k+1)} = \omega_{i,j}^{(k)} + \Delta t \Bigg[\Delta y^2 \omega_{i-1,j} + \omega_{i+1,j}\big(\Delta y^2 - Re\Delta x \Delta y^2 u_{i,j}\big) + \Delta x^2 \omega_{i,j\pm1} + \dots$$

$$\dots + \omega_{i,j\mp1}\big(\Delta x^2 \pm Re\Delta y \Delta x^2 v_{i,j}\big) + \omega_{i,j}\Big(\mp Re\Delta y \Delta x^2 v_{i,j} + Re\Delta x \Delta y^2 u_{i,j} - 2\Delta y^2 - 2\Delta x^2 \Big) \Bigg]$$

The k index stands for the iteration number taken until reaching convergence criterion. The time step however, could be conveniently extracted using *Brauer's Theorem* for a 2D problem, when mesh steps' are equal :

$$\Delta t \leq \min \left\{ \frac{1}{\frac{|u_i|}{\Delta x} + \frac{|v_j|}{\Delta y} + \frac{4}{Re\Delta x \Delta y}} \right\}_{\Delta x = \Delta y} \qquad \forall \qquad \begin{cases} i = 1,\ \dots,\ N \\ j = 1,\ \dots,\ M \end{cases} \tag{4.6}$$

Later we'll see that equal step sizes approach <u>is not</u> fully compatible with our specific problem since the geometry imposes $x - y$ ratio that takes a heavy computational cost. Therefore an empirical optimization approach of Δt vs. (Δx, Δy) will be held.

5 Influence of the numerical methods

In this chapter I will elaborate on the numerical tuning process, and the optimal values eventually taken. The comprehensive examination of the chosen method's influence is a tough task for the high number of degrees of freedom. The best I could was to take a "frozen" case with some constant parameters, and commence an optimization process in sought of optimality.

5.1 Convergence criterion

Given four different functions that are evolving from initial condition into steady state, one must verify that each consecutive difference reaches steady-state :

$$[u^{(n+1)} - u^{(n)}, v^{(n+1)} - v^{(n)}, \psi^{(n+1)} - \psi^{(n)}] < \epsilon \tag{5.1}$$

And since iterative convergence might not be obtained for the big sizes of ω at some specific points, it is advised to use the following criterion (and check every few iterations) :

$$\left| \frac{\omega^{(n+1)} - \omega^{(n)}}{\omega_{max}} \right| < \epsilon \tag{5.2}$$

The trade-off between the mesh resolution and Δt was examined along that chapter, and many cases were avoided for their impossible computational time. The first step I did was defining equal step sizes ($\Delta x = \Delta y \Leftrightarrow \Delta l$), and examining the duration w.r.t convergence size ($10^{-5} \leq \epsilon \leq 10^{-2}$). Smaller sizes were simply impractical to be calculated, as they generate matrices with 10^6 cells, and higher.

The next figure shows a set of tests in order to examine how the execution responds to different convergence criteria, and to the mesh density.

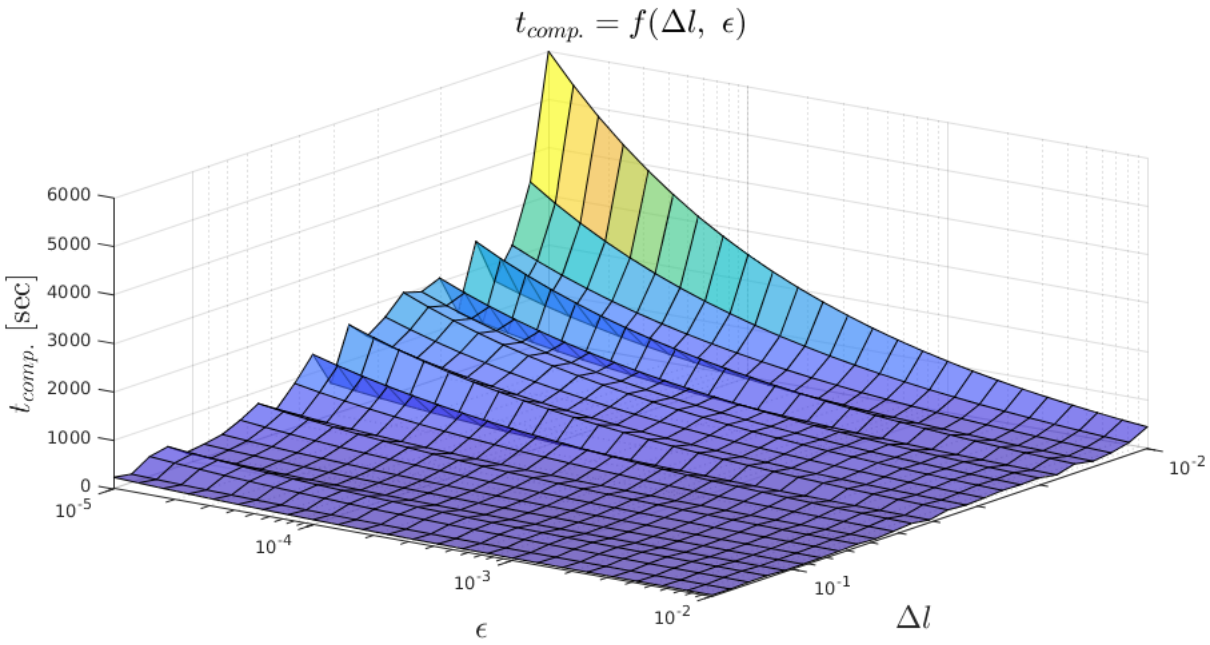

Figure 3: Computational time vs. $(\Delta l,\ \epsilon)$

We can see that computation cost rises sharply as $(\epsilon,\ \Delta l)$ get smaller, and vice versa. Note that Δl has an upper bound of 0.5/3 which is the minimal number of cells required for the orifice width (*red*). Smaller sizes "freeze" the calculation process :

	1	2	3	4	5	6	7	8	9
1	0	0.0405	0.1440	0.2835	0.4320	0.5625	0.6480	0.6480	NaN
2	0	-72.8345	-127.8782	-153.6858	-147.6457	-114.3476	-62.0813	0.6480	NaN
3	0	-163.4801	-285.2224	-339.6193	-323.1407	-248.3492	-134.5226	0.6480	NaN
4	0	-295.7888	-510.0339	-596.7439	-557.0577	-421.5086	-226.3795	0.6480	NaN
5	0	-509.6845	-862.4807	-979.8614	-887.4716	-654.3954	-346.0529	0.6480	NaN
6	0	-878.7231	-1.4521e...	-1.5747e...	-1.3577e...	-962.5086	-496.5426	0.6480	NaN
7	0	-1.5487e...	-2.4908e...	-2.5071e...	-2.0083e...	-1.3422e...	-666.0899	0.6480	NaN
8	0	-2.7762e...	-4.4589e...	-3.9583e...	-2.8253e...	-1.7311e...	-811.9798	0.6480	NaN
9	0	-4.1944e...	-8.6095e...	-6.0420e...	-3.6042e...	-1.9453e...	-845.3140	0.6480	NaN
10	0	-4.1467e...	-1.9001e...	-8.1751e...	-3.6116e...	-1.6006e...	-624.3866	0.6480	NaN
11	0	0.6480	0.6480	0.6480	0.6480	0.6480	0.6480	0.6480	NaN
12	0	0.6480	NaN	NaN	NaN	NaN	NaN	NaN	NaN
13	0	0.6480	NaN	NaN	NaN	NaN	NaN	NaN	NaN
14	0	0.6480	NaN	NaN	0.6480	0.6480	0.6480	0.6480	0.6480
15	0	0.6480	NaN	NaN	0.6480	2.0418e...	3.7097e...	4.8280e...	5.3988e...
16	0	0.6480	NaN	NaN	0.6480	4.4503e...	7.9691e...	1.0203e...	1.1237e...
17	0	0.6480	NaN	NaN	0.6480	7.7708e...	1.3513e...	1.6780e...	1.7983e...
18	0	0.6480	NaN	NaN	0.6480	1.3073e...	2.1533e...	2.5420e...	2.6130e...
19	0	0.6480	NaN	NaN	0.6480	2.2860e...	3.4125e...	3.7238e...	3.6097e...
20	0	0.6480	NaN	NaN	0.6480	4.3835e...	5.4870e...	5.3309e...	4.7879e...
21	0	0.6480	0.6480	0.6480	0.6480	9.5954e...	8.8211e...	7.3248e...	6.0291e...
22	0	-5.5474e...	5.1770e...	1.0161e...	4.4450e...	2.1105e...	1.2878e...	9.1179e...	6.9957e...
23	0	-4.8088e...	-4.2771e...	2.4427e...	2.4684e...	1.7579e...	1.2468e...	9.2732e...	7.2215e...

Figure 4: Insufficient number of cells at the orifice

For practical runtimes, I chose convergence size of $\epsilon < 10^{-3}$, which will be shortly justified.

5.2 Optimal parameters

In this subsection I conducted a comparison between different parameters w.r.t computation time until reaching **steady-state**.

After setting ϵ's size, I made a set of tests in sought of convenient $\Delta x/\Delta y$ ratio, that will suit practically to the geometry of the problem. The long length at x-axis (=L) should be handled differently than that of y-axis, which is shorter. Moreover, the orifice is very thin (=L/40), and thus generates lots of reactions that we would like to focus on.

The best ratio was found to be $\Delta x/\Delta y = 5$, and its size is simply notated as Δl. The next figure exhibits a long lasting empirical tests in sought of optimal **computation time** (z-axis), and the grey-scale colorbar (=right) shows the **number of iterations**.

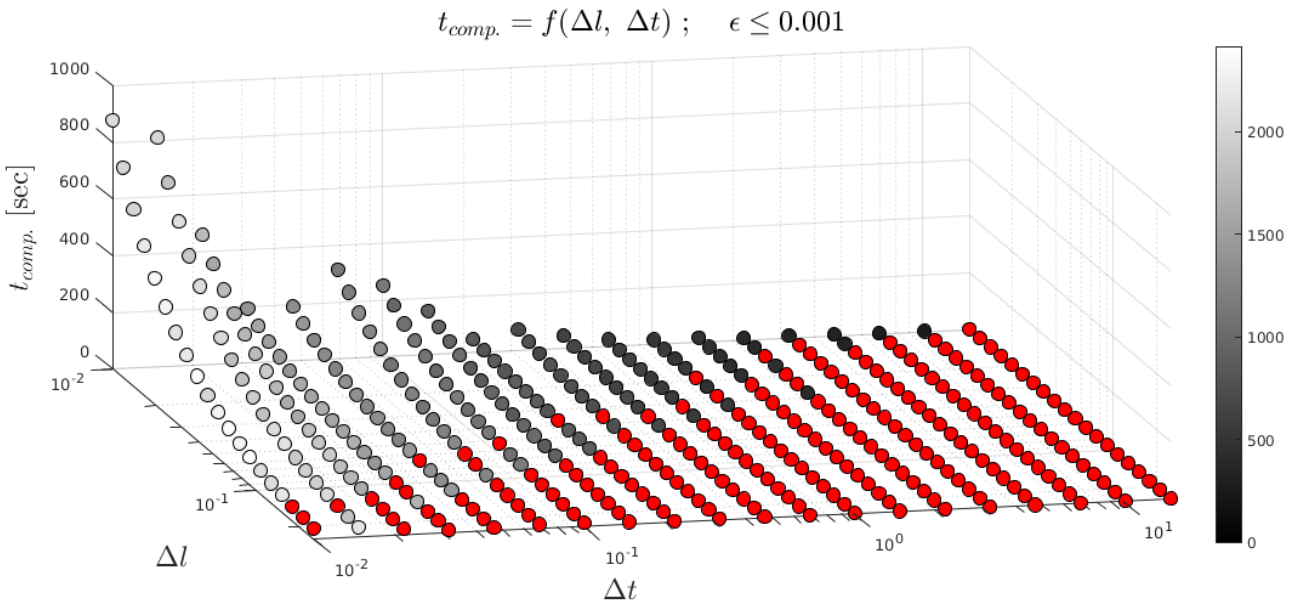

Figure 5: Optimal region obtained via parameter space

Note that only grey-scale points stand for converged executions, while *red* points represent diverged executions that were ignored. Anyway, we can see an interesting relation between $(\Delta l,\ \Delta t)$. As the grid turns denser the computation time rises sharply ($\Delta l \downarrow : t_{comp.} \uparrow$), but more cases manage to converge. But as we relieve the mesh size, the computation time reduces drastically ($\Delta l \uparrow : t_{comp.} \downarrow$), and convergence is less guaranteed unless smaller time steps are used. Additionally, too big time steps ($\Delta t \uparrow$) resulted also in divergence, failing to restrain the vorticity gradient : $\omega^{k+1} = \omega^k + \nabla\omega^k \Delta t$.

The grey-scale **face-color** of the points represent the amount of iterations needed to reach steady-state. In this case, the greater the time step, the shorter the computation time ($\Delta t \uparrow : t_{comp.} \downarrow$). The reason is understandable since greater time steps accelerate the progression rate. The following figures demonstrate some of the edge cases :

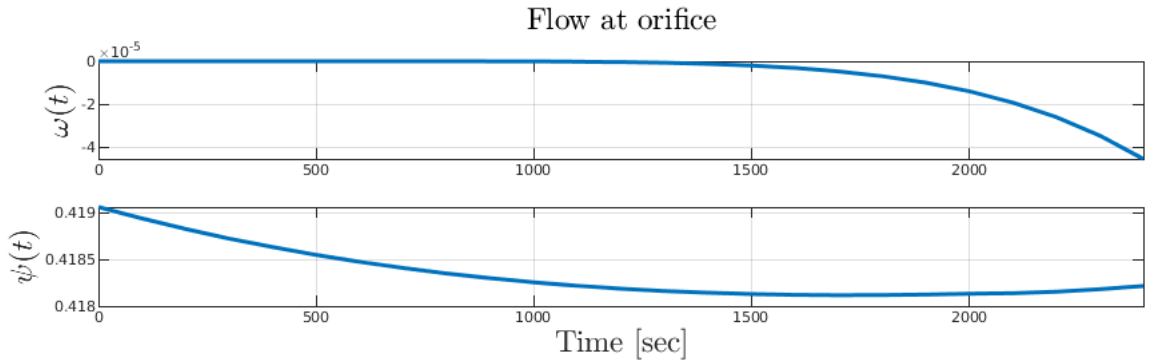

Figure 6: Too small Δt results in insufficient progression

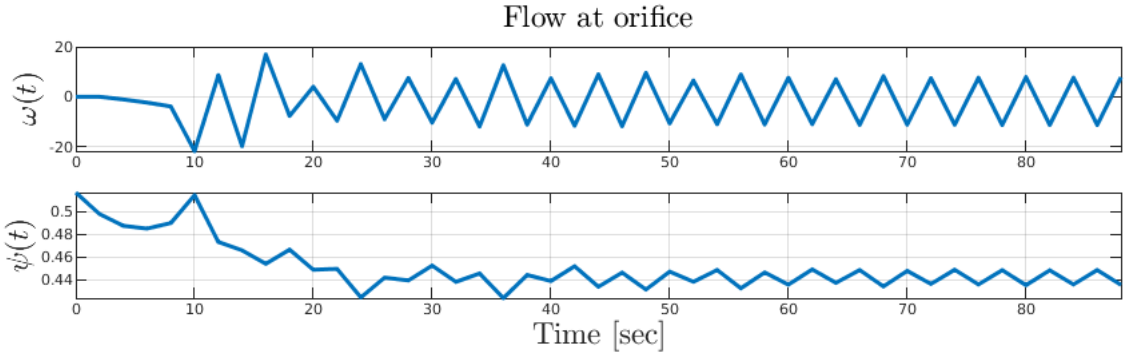

Figure 7: Slightly big Δt results in unstable fluctuations

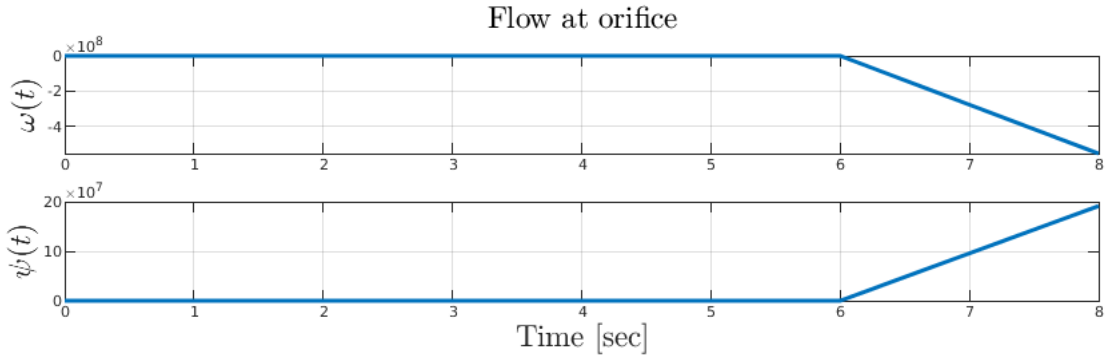

Figure 8: Too big Δt results in rapid divergence

However, values in the permissible region exhibited in fig. 5.2 perform well within a reasonable amount time, either by t and $t_{comp.}$:

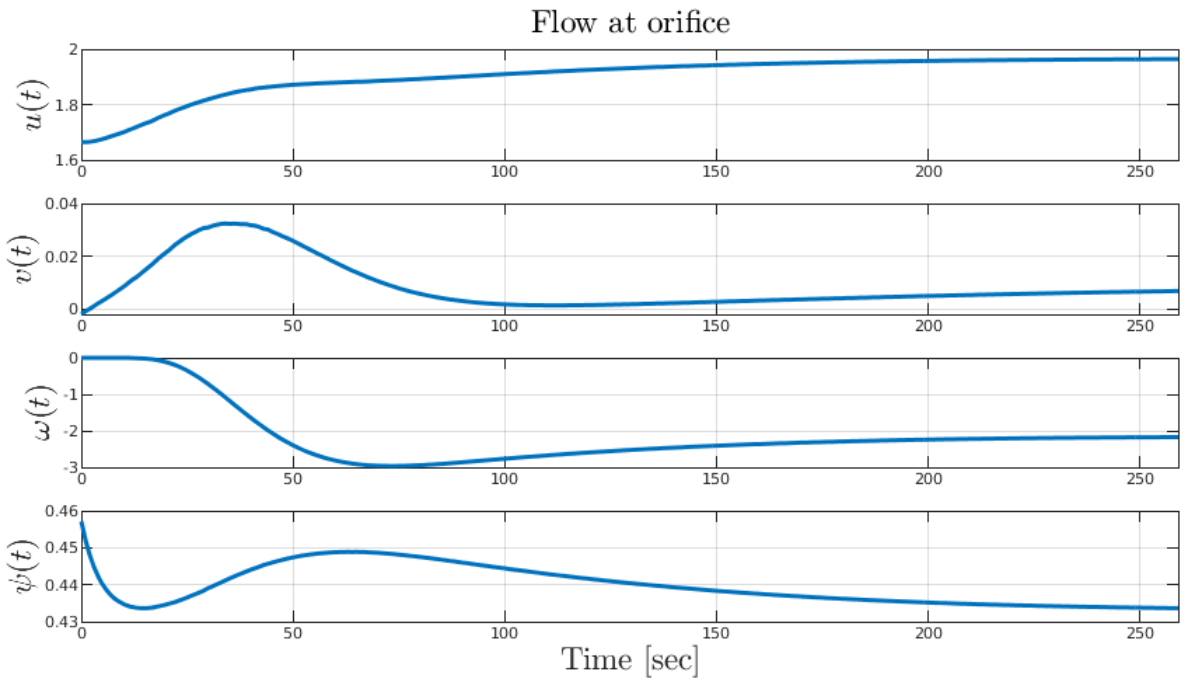

Figure 9: Example of succesfull set of parameters within permissible range

We can see a "healthy" shape of a dynamic response decaying towards a stable steady-state, under a sufficient convergence criterion. Note that values were not taken from "0" initialization, but from 2nd iteration for numerical reasons.

So now we are ready to move on to the results section, presenting a comparison for two case studies : $Re = [100, 750]$. The results are comprised of u, v, ψ, ω and the dynamic response of each of them, until reaching steady state. The chosen parameters were obtained using the mentioned above analysis :

$$\epsilon = 10^{-3} \qquad \Delta t = 0.831 \qquad \Delta y = \Delta x/5 = 0.04$$

$$[M,\ N] = [\frac{L}{\Delta x} + 1, \frac{6L/20}{\Delta y} + 1] = [101, 151]$$

$$\textbf{S.O.R :}\ \ [\Omega_{opt},\ \mu] = [1.949, 0.997]$$

6 Results

Starting off with a high level sight of the time dependent response of both cases :

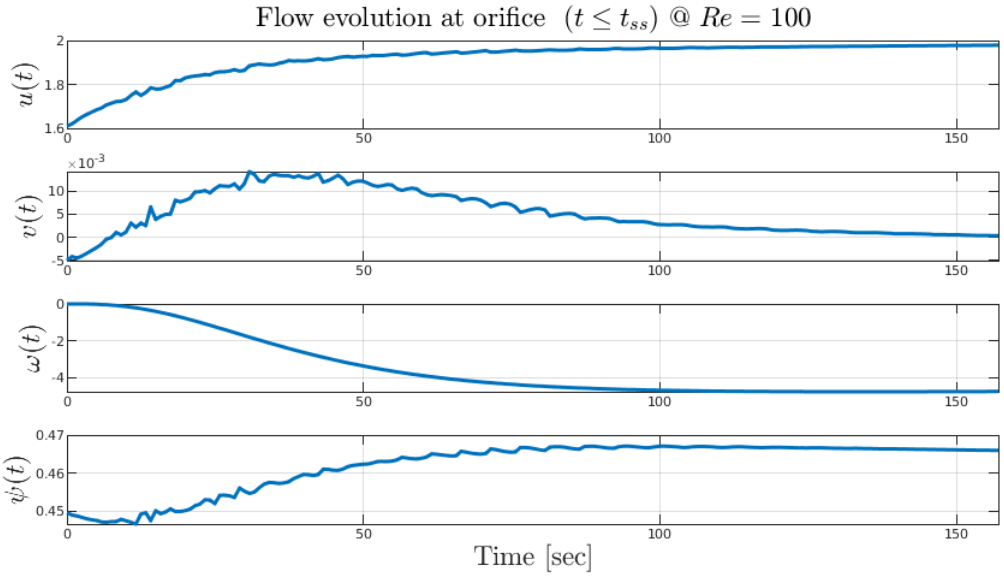

The lower Reynolds reaches steady state faster than higher values ($t_{ss}^{100} < t_{ss}^{750}$), but is also subjected to stronger influence of the time interval, shown by the fluctuated spikes.

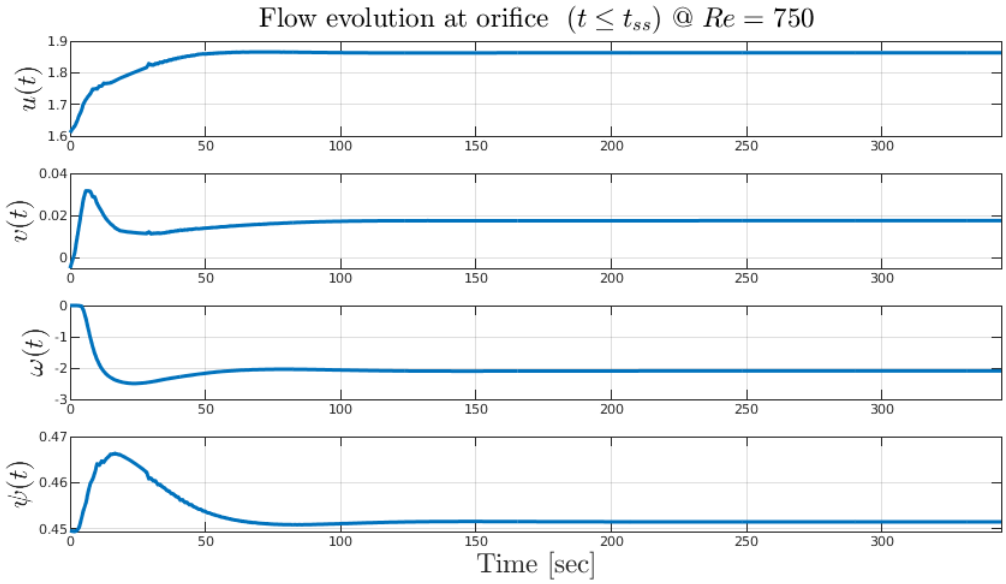

Higher Re exhibits sort of an "overshoot" that after a while is restrained and stability seems to be obtained quicker, but convergence lasts longer.

I added *Matlab*'s streamlines option such that the contour lines can better demonstrate the concentration gradient. However, **horizontal velocity** varies widely w.r.t the Re number:

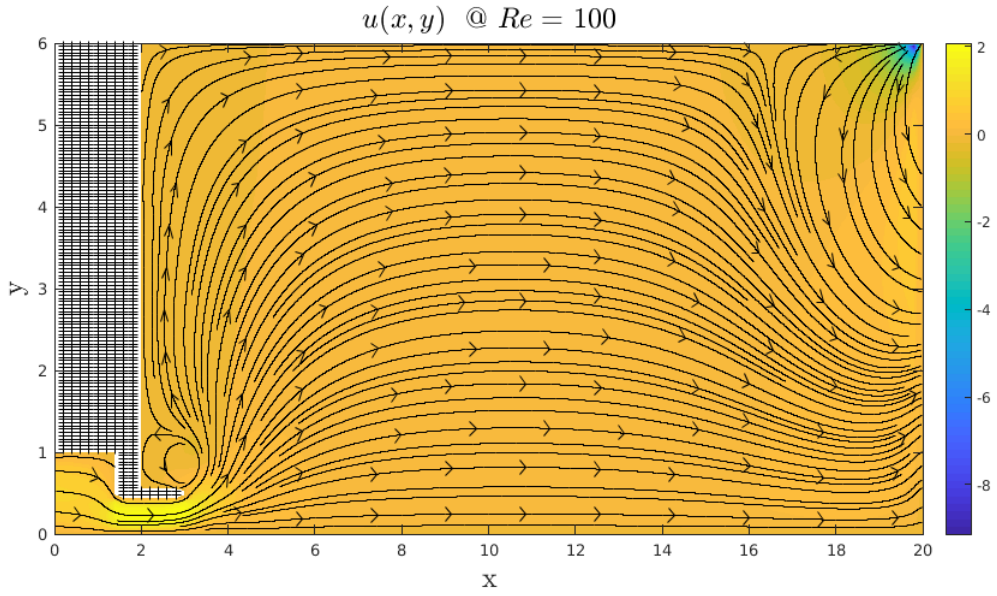

Low Re exhibits an expected behavior of u increase as the cross-section narrows (*yellow*), and the streamlines perform a "calm" disperse after leaving the orifice contraction.

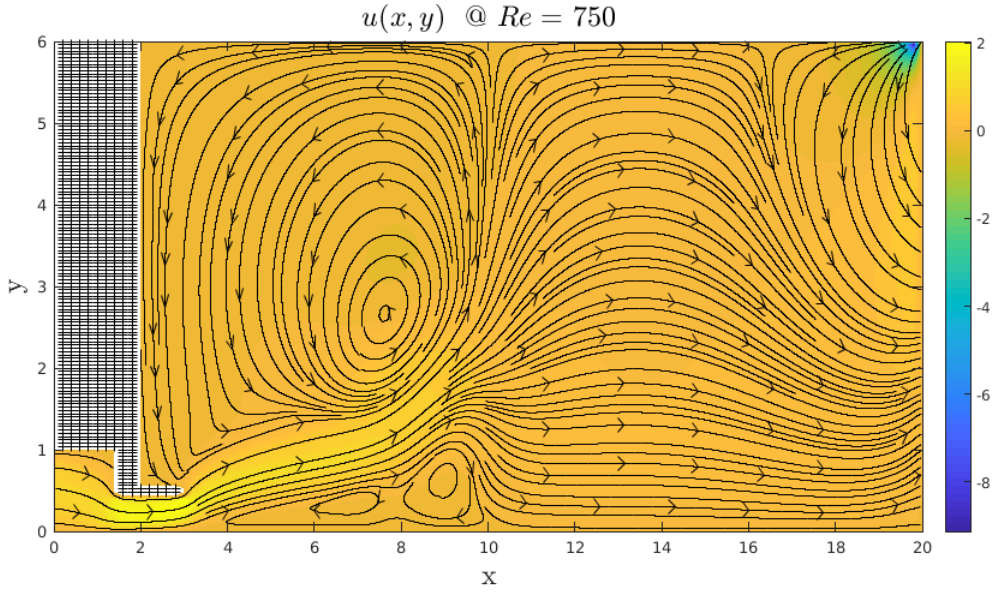

High Re exhibits a more aggressive policy as the flow remains high, long atfer leaving the orifice. The streamlines as well perform higher rates of vorticity causing few local turbulences across the plane, and next to the walls.

The **vertical velocity** behaves entirely different since the incoming velocity is completely horizontal and only does the geometrical constraints, exert $u \to v$.

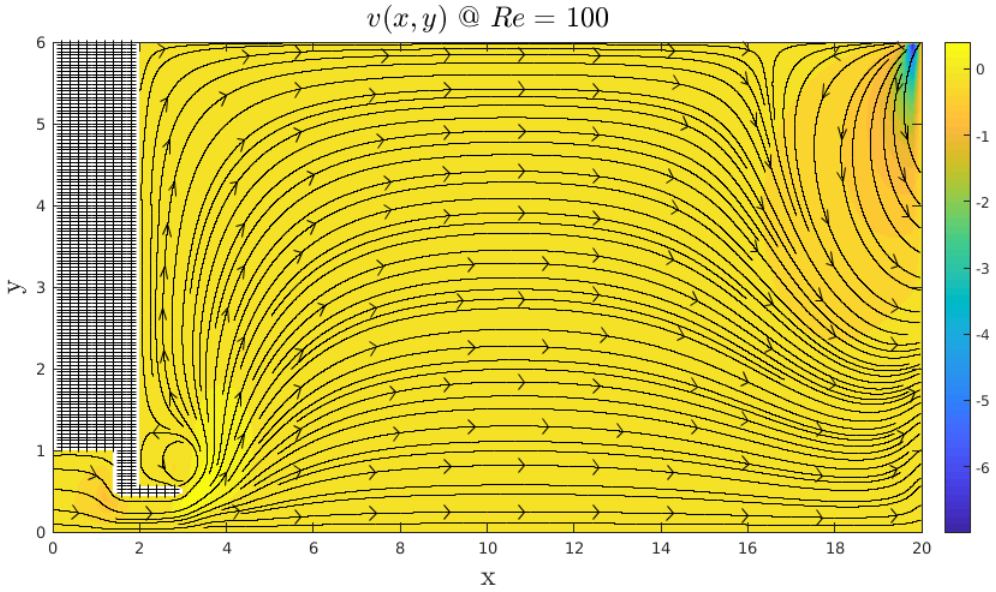

Low Re number manages to conserve u component as seen either by the *yellow* color level and by the dominant horizontal streamlines ($v \approx 0$).

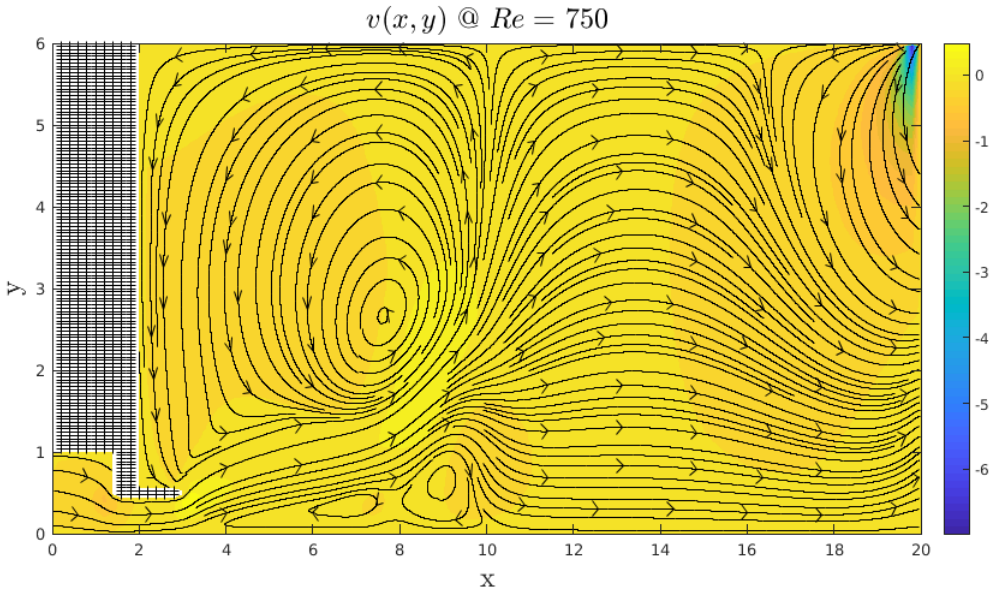

However, when Re grows, turbulent policy is observed above the orifice and towards the exit. The vertical component becomes lively *orange* wherever turbulences are formed.

The overall **vorticity** is calculated in two manners : Boundary layers on the walls, and inner flow (further away). Inner flow is calculated by a $\nabla\omega^k\Delta t$ increment, which remains low relatively to the boundary layers, and high values developed mainly in the orifice exit :

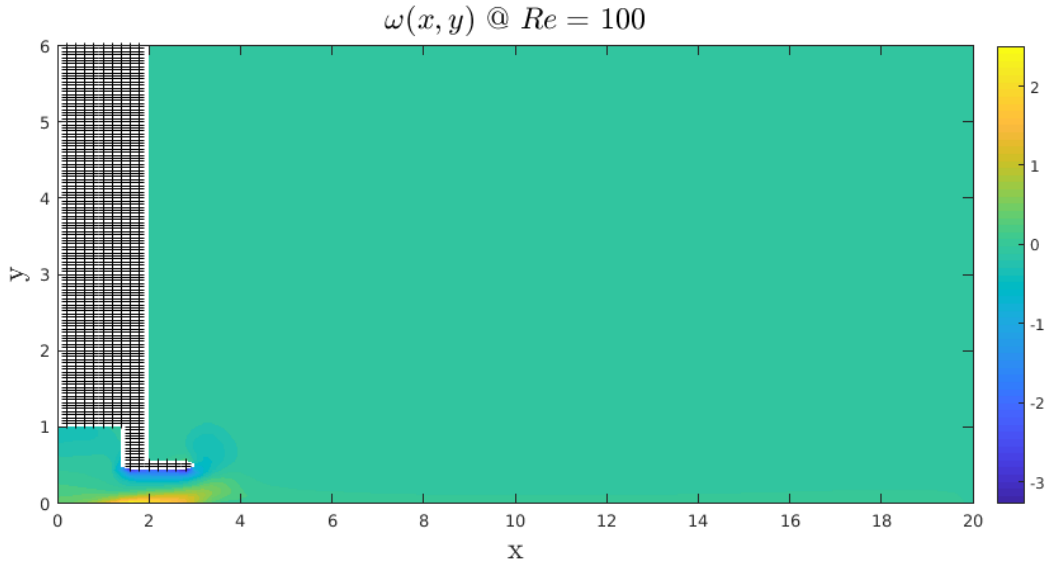

The reason for the dominant *green* color is that all across the shape, low values of vorticity are developed. Contrarily, the contraction effect of the orifice accelerates the stream, which in turn generates turbulences along the walls ($\neq$ *green*). Note that the parallel walls generate opposite colors, symbolizing the opposite direction of the vorticity.

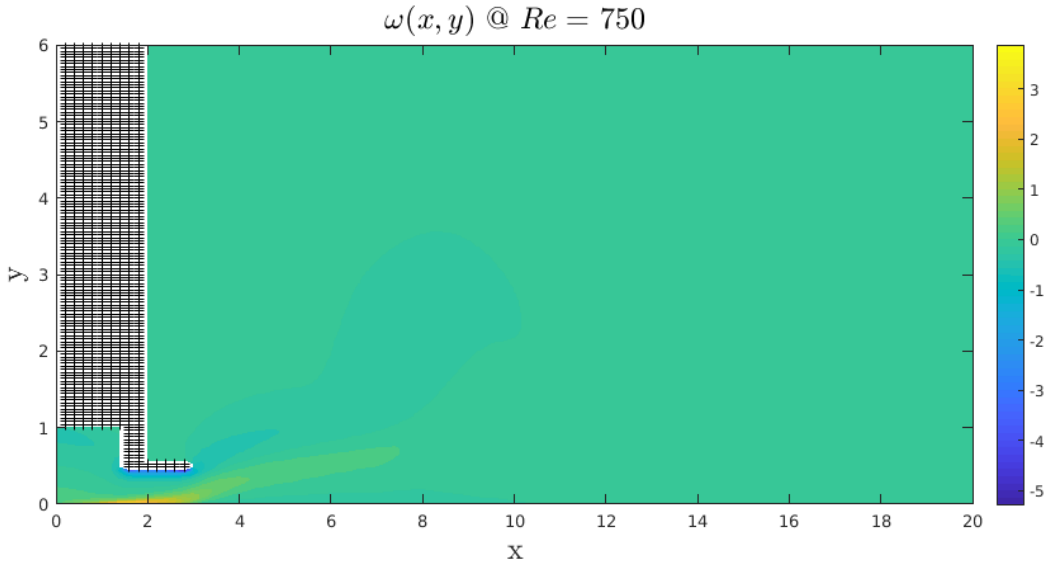

A close up look on the orifice might sharpen that :

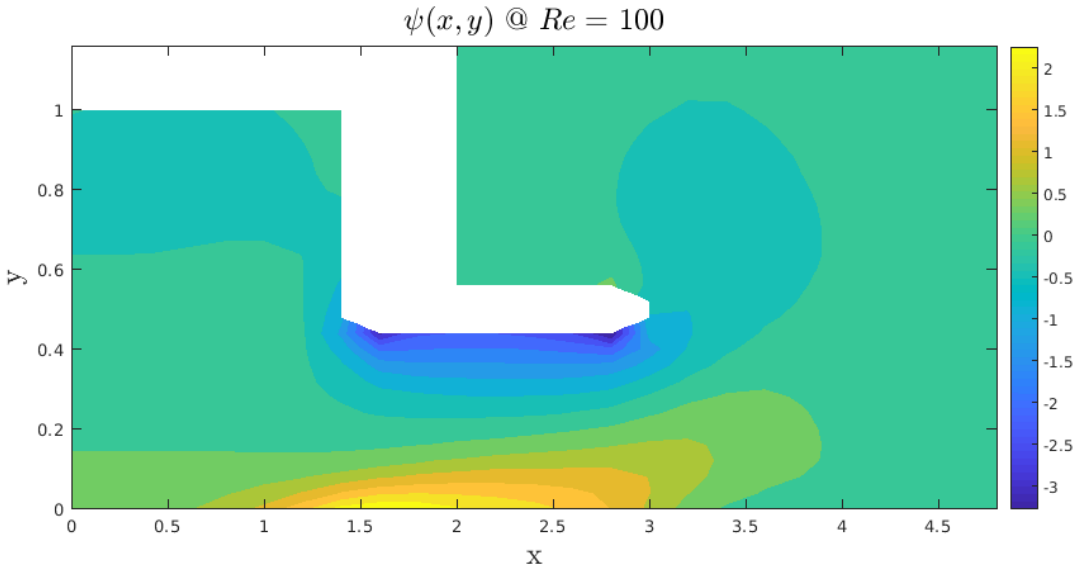

The reason for the colorful distribution on almost zero (*green)* background, is that boundary layer is calculated w.r.t the velocity field :

$$\omega_{i,\mathrm{w}} = 2 \cdot \frac{\psi_{\mathrm{w}\pm\Delta x} - \psi_{i,\mathrm{w}}}{\Delta y^2} + O(\Delta x)$$

Such that high values are expected to form wherever the difference (numerator) is big :

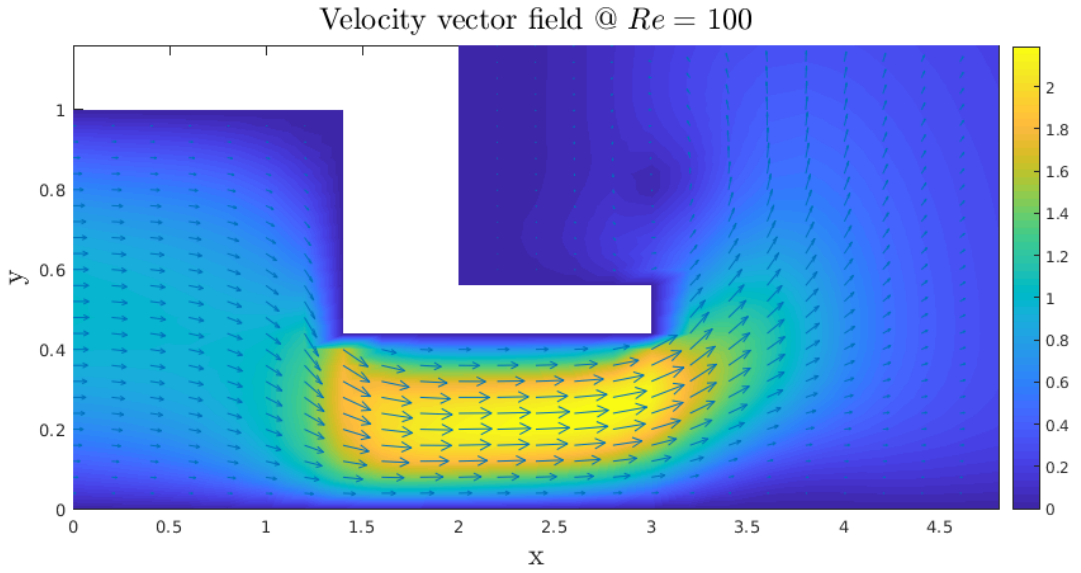

And now we shall examine the most important solution obtained form the execution.

The following figures show the **stream** function obtained from the boundary conditions and the inner field. As seen colorfully, their upmost points satisfy section **3.2**: $[\psi_{in}(1),\ \psi_{out}(6)] = [\frac{2}{3},\ 3\frac{1}{3}]$. And an integral on both profiles yields equivalence between total input and output, and thus fulfills conservation condition.

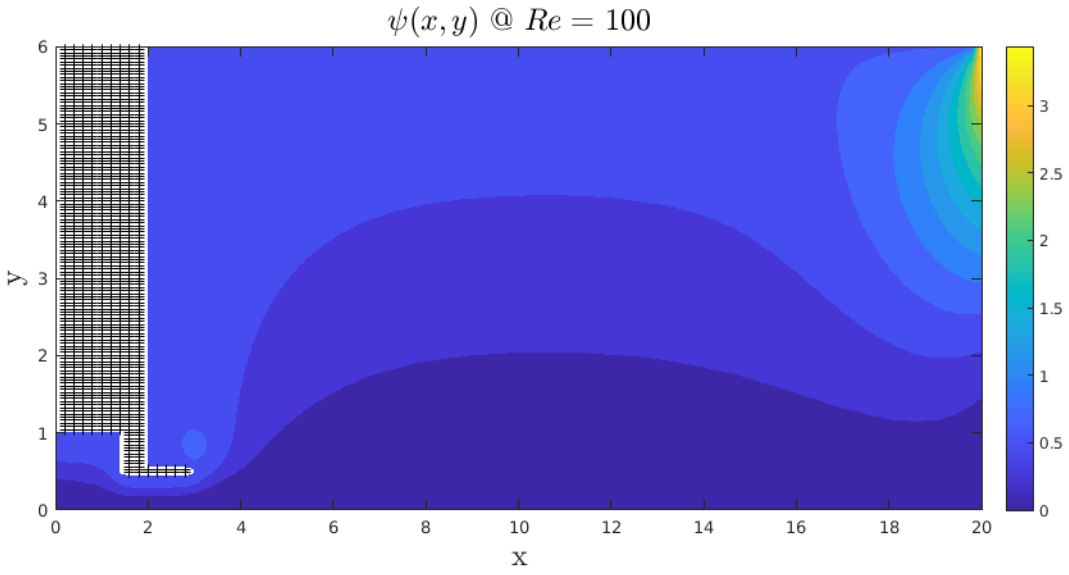

Low Re shows subtle contour lines that correspond to the stream lines we have just seen. Soft turbulences allow wide dispersion that seems to divide equally to three value levels.

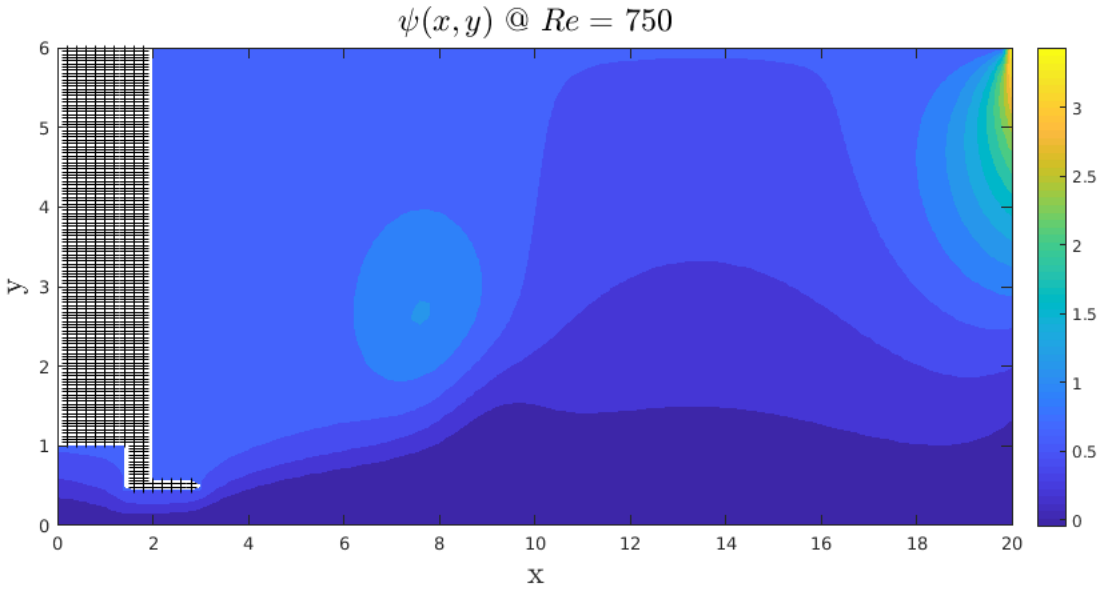

High Re evokes higher ψ values alongside turbulences in the shape's center and the outlet.

In order to get a better insight on the **orifice** region, I performed a close up examination :

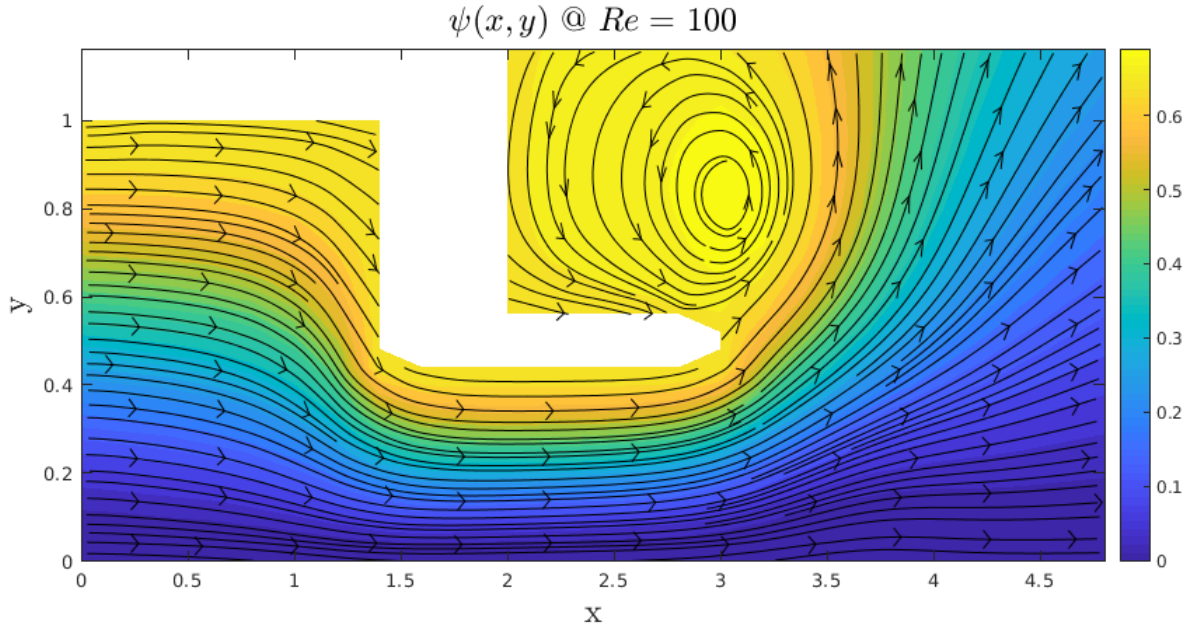

Note that colorbar was re-normalized due to change of interest zone. The low Re allows flow to follow the walls right after exiting the orifice, and generate circulation.

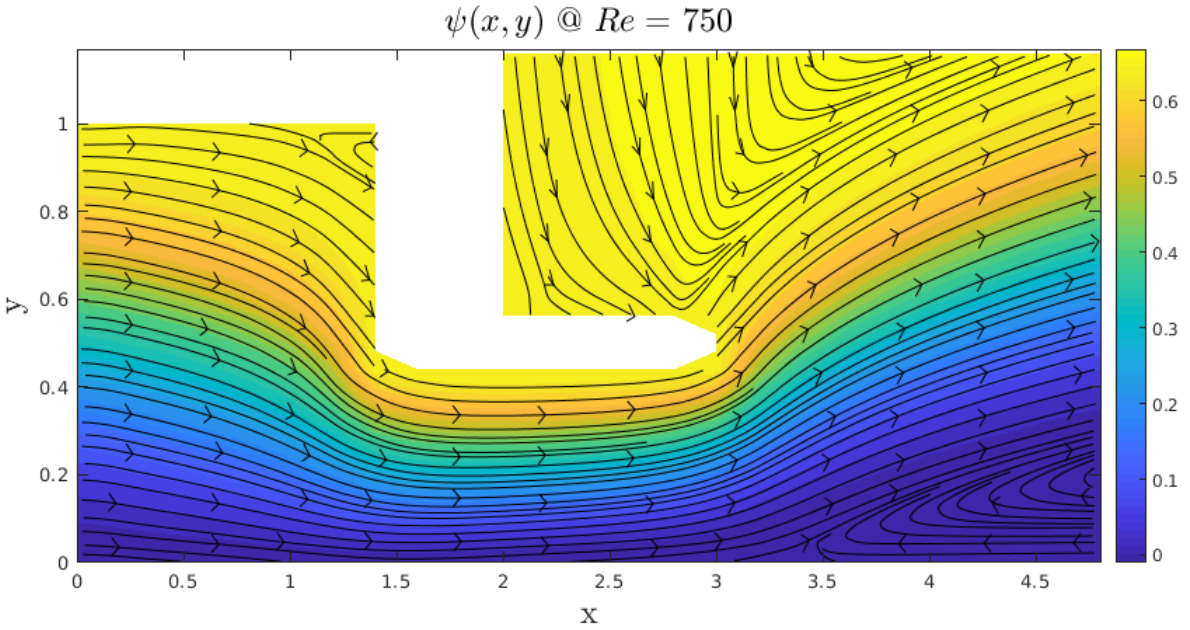

When Re is higher, the circulation is "postponed" to the center of shape, preventing the smooth tracing of the streamlines along the walls. Eventually, as a sanity check, I wanted

to make sure that the numerical calculations do comply with the fully developed flow formulation on section **3.2**. Expectedly, showing parabolic velocity distribution :

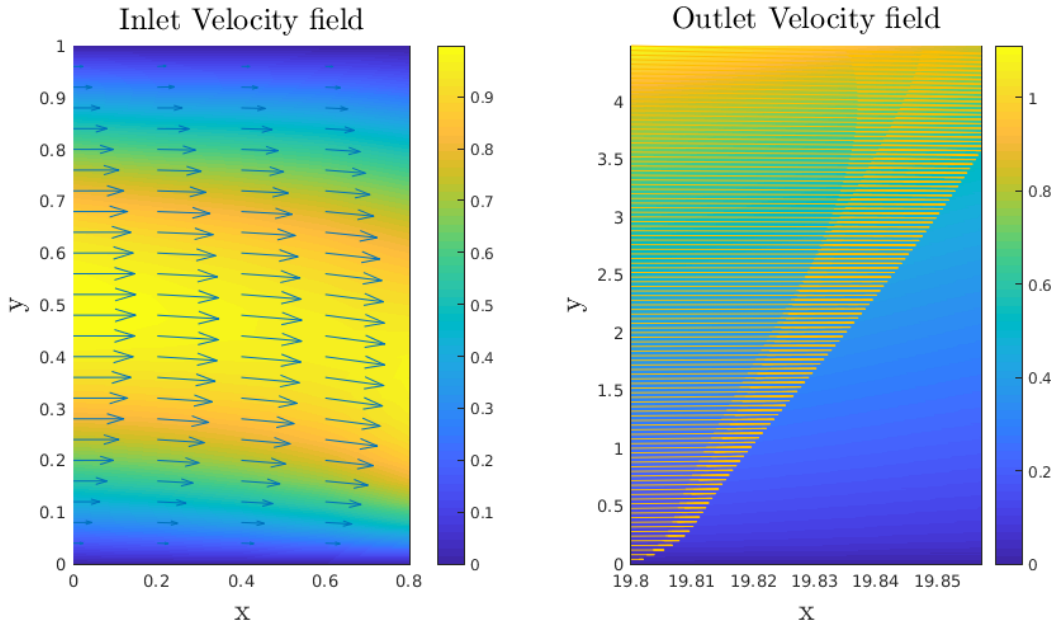

6.1 Comparison between Re numbers

The Last results section will show the function difference between $Re_{(100)} - Re_{(750)}$:

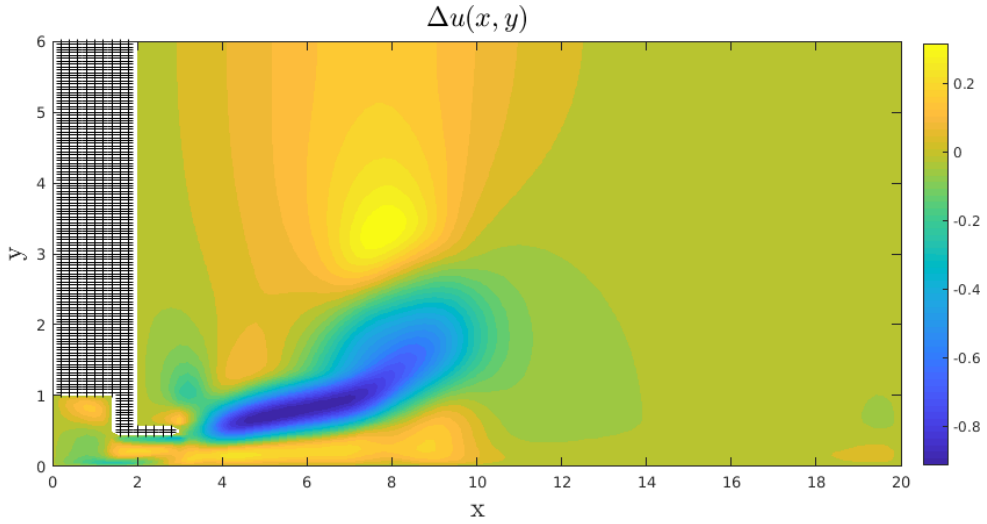

The color difference denotes the change that the $\underline{\underline{Re = 750}}$ generates. That means that negative u (*blue*) is due to decrease in horizontal velocity and vice versa (*yellow*=increase).

Here we can see clearly that higher Re evoke "singular" circulations across the center. Either here, the color's temperament corresponds to the direction coerced by the proximity to the walls. And as the fluid advances, the circulation happens to grow bigger.

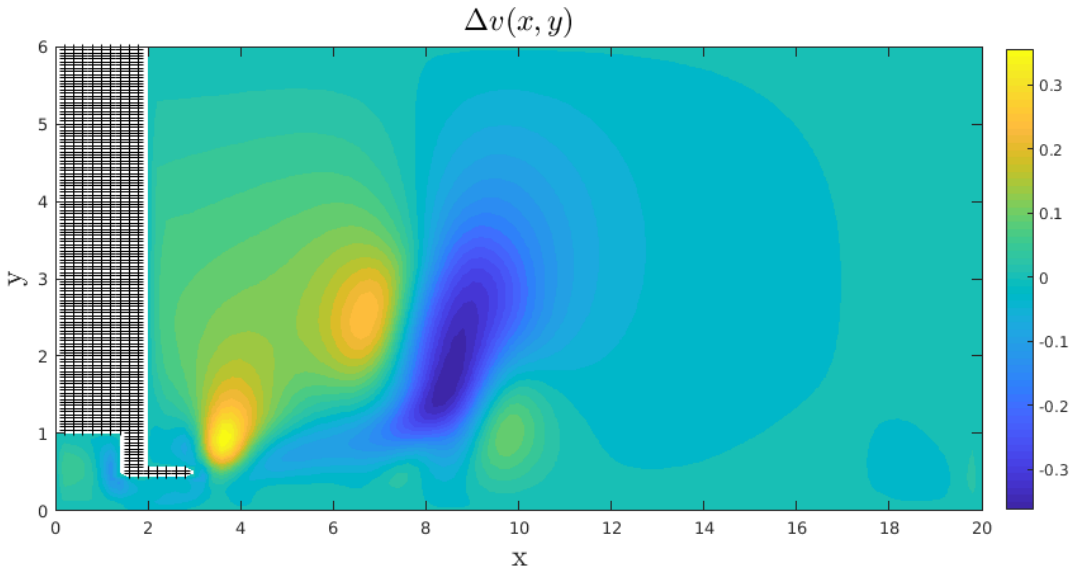

Similarly to the **vorticity** figure we have already seen, the difference goes either here in small numbers, but points on the suspicious area - the orifice exit.

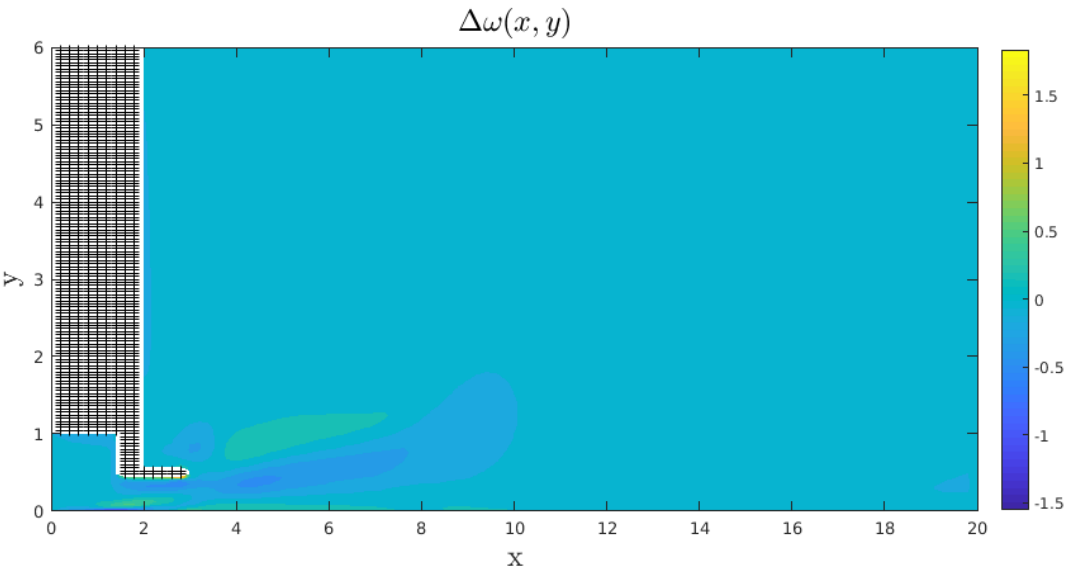

Higher Re leads to a more aggressive turbulence.

And most important, the stream difference. Beside few areas showing positive stream difference (*yellow*), almost all the areas in the shape show negative values, meaning that the flow regime turns opposite after a certain critical Re value.

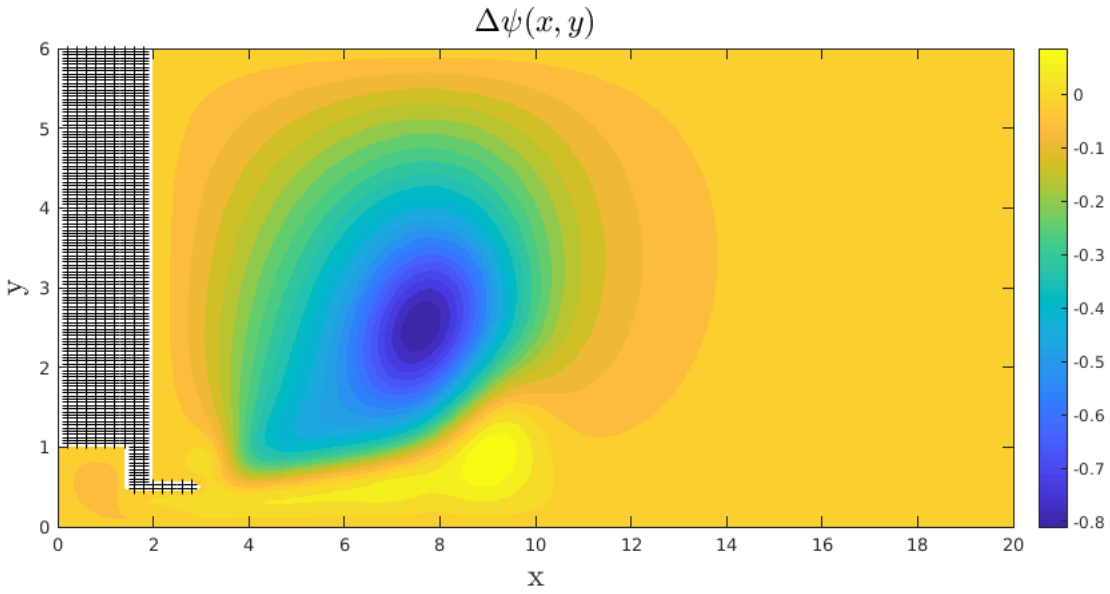

7 Summary and conclusion

• We saw a reasonable match between the theoretical development at class and notebook, and the obtained results.

• The problem was solved using *1st order upwind differences* for the vorticity and *Gauss-Seidel & SOR* for the stream function.

• The boundary conditions were not fully defined for sharp corner points, where high vorticity was forced by the acute change of the flow direction.

• The flow further away from the walls, can be said to be laminar as long as Re kept small.

• The optimization stage showed indifference to different Reynolds values.

• Using *1st order upwind differences* helped simplifying the implementation of the technical stage, that was already prone to obstacles.

• The author has encountered **tons** of technical challenges along the was but never gave up, despite poor understanding and intuition in Fluid mechanics.

In these very last words, I hereby would like to thank you *Barry*, and to thank myself *Daniel*, for not giving up, although last year I left in the middle of the semester, unable to keep pace with class. So finally, I can dismiss the numerical relief :

(!) **S**uccessive **O**ver **R**elaxation (!)

$-\ fin\ -$